The effect of phase heterogeneity on thermoelectric properties of nanostructured silicon germanium alloy

Zahra Zamanipour, Erfan Salahinejad, Payam Norouzzadeh, Jerzy S. Krasinski, Lobat Tayebi et al.

Citation: J. Appl. Phys. **114**, 023705 (2013); doi: 10.1063/1.4813474
View online: http://dx.doi.org/10.1063/1.4813474
View Table of Contents: http://jap.aip.org/resource/1/JAPIAU/v114/i2
Published by the AIP Publishing LLC.

The effect of phase heterogeneity on thermoelectric properties of nanostructured silicon germanium alloy

Zahra Zamanipour,[1] Erfan Salahinejad,[2] Payam Norouzzadeh,[1] Jerzy S. Krasinski,[1] Lobat Tayebi,[2,3,a)] and Daryoosh Vashaee[1,a)]
[1]*School of Electrical and Computer Engineering, Helmerich Advanced Technology Research Center, Oklahoma State University, Tulsa, Oklahoma 74106, USA*
[2]*School of Material Science and Engineering, Helmerich Advanced Technology Research Center, Oklahoma State University, Tulsa, Oklahoma 74106, USA*
[3]*School of Chemical Engineering, Oklahoma State University, Stillwater, Oklahoma 74078, USA*

(Received 16 April 2013; accepted 19 June 2013; published online 11 July 2013)

Detailed examination of the nanostructured bulk $Si_{0.80}Ge_{0.20}$ alloy synthesized by mechanical alloying and hot-press methods revealed that the alloy composition can unintentionally deviate from its nominal value. The phase deviation is difficult to be detected with x-ray diffraction due to the continuous solid solution characteristics of the Si-Ge alloy. Differential thermal analysis, in particular, showed that the synthesized nanostructured bulk $Si_{0.80}Ge_{0.20}$ alloy was a composition of two unintentional phases. The dominant phase was $Si_{0.88}Ge_{0.12}$ with admixture of $Si_{0.58}Ge_{0.42}$ in a much lower concentration. The two-phase structure is difficult to be detected in X-ray diffraction analysis and is often neglected. Thermoelectric properties of $Si_{1-x}Ge_x$ significantly depend on the Ge content in the synthesized alloy. The thermoelectric properties of the synthesized material were studied experimentally and theoretically. The comparison of the data of the mixed phase nanostructured alloy with those of the single phase $Si_{0.80}Ge_{0.20}$ alloy showed enhancement in Seebeck coefficient and reduction in thermal conductivity of the former material. It was found using model calculations that these differences are due to the existence of the $Si_{0.88}Ge_{0.12}$ phase in the two-phase structure that results in the reduction of the bipolar diffusion part of the thermal conductivity and the bipolar effect in the Seebeck coefficient at high temperature. The results can stimulate a new route for enhancing the thermoelectric properties of silicon germanium alloy based on multicomponent material design. © *2013 AIP Publishing LLC*. [http://dx.doi.org/10.1063/1.4813474]

INTRODUCTION

Thermoelectric properties of silicon germanium alloys have been studied extensively over the last several decades for high temperature power generation applications mainly for Radioisotope Thermoelectric Generators (RTGs).[1] Along with its superior thermoelectric properties, silicon germanium has the desired physical and mechanical properties such as high melting point, low vapor pressure, and resistance to atmospheric oxidation.

Bulk nanostructuring has been recently applied to several thermoelectric materials to enhance their thermoelectric conversion efficiency.[2] The dominant effect of bulk nanostructuring is the reduction of the lattice thermal conductivity. Bulk nanostructured materials contain a high concentration of interfaces that enhance the phonon scattering and reduce the lattice thermal conductivity. Nanostructuring has been also recently applied to silicon germanium which has resulted insignificant enhancement of the thermoelectric figure-of-merit (ZT).[3–10] It has been shown that bulk nanostructuring does not always result in the enhancement of the figure-of-merit. For the ZT enhancement to happen, it is essential that the phonon mean free path be significantly larger than both the grain size and the electron mean free path, which is satisfied in nanostructured silicon germanium due to the large mean free path of the dominant phonons.[11,12]

The thermal behavior of $Si_{1-x}Ge_x$ alloys has been studied theoretically.[13–15] There are several parameters such as Ge concentration, doping concentration, and temperature which affect the thermal properties of this material system. Due to the strong phonon scattering by point defects resulted from alloying with Ge, Ge content plays an important role in lattice thermal conductivity.[16–18] While the increase of the Ge content up to approximately 50% decreases the lattice thermal conductivity, it also reduces the band gap that consequently increases the ambipolar diffusion part of the thermal conductivity. This part becomes comparable or higher than the lattice part of thermal conductivity at high temperature.[3] Previous experimental[17,19] and theoretical reports[15] have shown that the lattice thermal conductivity is approximately at its minimum value at 12% Ge content. Further increase of Ge concentration does not noticeably reduce the lattice thermal conductivity, but the ambipolar thermal diffusion increases significantly and dominates at high temperature. Nevertheless, $Si_{0.7}Ge_{0.3}$ and $Si_{0.8}Ge_{0.2}$ have been the most common material compositions studied and applied for thermoelectric power generation.[1]

It can be concluded that precise knowledge of the structural phases of the synthesized $Si_{1-x}Ge_x$ alloy would help to analyze the experimental data and guide the experiments to adjust the process parameters for achieving the desired Ge

a)Authors to whom correspondence should be addressed. Electronic addresses: lobat.tayebi@okstate.edu and daryoosh.vashaee@okstate.edu.

concentration in the alloy. Therefore, in order to analyze and optimize the thermoelectric properties of the $Si_{1-x}Ge_x$ alloy, the Ge content must be precisely measured.

The X-ray diffraction (XRD) analysis has been the main characterization method for determining the alloy composition. However, since Si and Ge make continuous solid solution, the XRD lines of the different phases overlap. The XRD data of nanostructured $Si_{1-x}Ge_x$ cannot precisely determine the phases due to the multiple numbers of unknown parameters such as the grain size, residual stress, instrumental broadening, and the phase heterogeneity. There has been little attention devoted to the phase determination of the nanostructured bulk $Si_{1-x}Ge_x$ thermoelectric alloys in the past. Differential thermal analysis (DTA) is one of the precise techniques that can show different transformations such as glass transitions, crystallization, melting, and sublimation in materials.[20] In DTA, the temperature of the sample is measured using a reference sample in the furnace while they are both receiving equal amount of heat. The area under the DTA peak gives the enthalpy change which is independent from the heat capacity of the material.[21] Therefore, DTA can be recognized as a reliable and accurate method for phase structure identification, especially for solid solutions where the XRD data can be difficult to be interpreted due to the infinite number of possible phases that can be formed. It would be of interest to determine the phase structure of the synthesized nanostructured $Si_{1-x}Ge_x$ alloy and study the corresponding thermoelectric properties using DTA.

The aim of the present manuscript was to identify the actual phase structure of the p-type nanostructured $Si_{0.8}Ge_{0.2}$ alloy synthesized via mechanical alloying and hot press sintering. XRD and DTA characterizations were performed on the synthesized material. Furthermore, the thermal properties along with transport properties of the material were analyzed and compared with those of the single crystalline alloy. The analysis revealed phase heterogeneity in the sample, which was not detected in the XRD data. This phase heterogeneity was responsible for the changes in the thermoelectric properties of the material.

EXPERIMENTAL PROCEDURE

Stoichiometric ratios of 80 at. % Si (99.9% purity), 20 at. % Ge (99.9% purity), and 1.6 at. % B (99.9% purity) were weighted and loaded into a tungsten carbide bowl with tungsten carbide balls under argon atmosphere. The powder was milled with Fritsch-P7 planetary ball mill for 10 h at 1000 rpm with ball to powder ratio of three. The powder was collected and annealed in a quartz crucible at 1100 °C for 3 h under argon atmosphere. The annealed powder was subsequently milled for approximately 60 h with same milling condition. The powder was then filled into a graphite die with an internal diameter of 12.7 mm and was hot pressed at 1200 °C for approximately 6 min under 108 MPa. The pressed sample was cut into rods and disks for thermoelectric properties measurements. The relative density of 93% of the theoretical density of $Si_{80}Ge_{20}$ (2.93 g/cm^3) was achieved.

The sample was characterized by XRD using Brucker AXS D8-Discover with Cu Kα radiation and scanning electron microscope (SEM, Hitachi S-4800). Seebeck coefficient and electrical conductivity were measured simultaneously with four probe technique by commercially available equipment (Ulvac ZEM-3) and the thermal conductivity was measured by a laser flash apparatus (Netzsch LFA 457) from room temperature to 950 °C. The DTA and thermogravimetric analysis (TG) were accomplished in argon environment by Netzsch STA 449 F1. The temperature was increased 20 °C per minute from room temperature to 1550 °C.

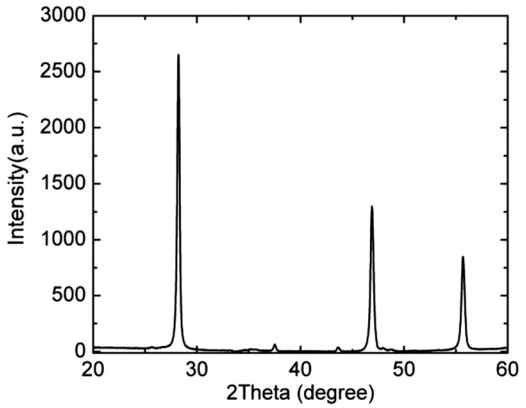

FIG. 1. X-ray diffraction pattern of the nanostructured silicon germanium sample.

RESULTS AND DISCUSSION

The XRD analysis of the sample is shown in Figure 1(a). As Si and Ge make a continuous solid solution alloy, the $Si_{1-x}Ge_x$alloy XRD peaks are located between Si peaks (with the main peak at $2\theta = 28.47°$) and Ge peaks (with the main peak at $2\theta = 27.29°$). The spectrum shows a single peak between the corresponding two peaks of Si and Ge indicating the formation of a homogenous composition alloy. The average crystallite size was estimated using Sherrer's equation.[22] In this equation, the instrument broadening was extracted and the residual stress of the sample was ignored. The average crystallite size of the sample was calculated to be 27 nm.

DTA, derivative of DTA (DDTA), and TG of the sample are shown in Figure 2. The DTA and DDTA curves show two endothermic events attributed to liquation of two different phases. Considering the Si-Ge phase diagram[23] and the endothermic peaks observed in the DTA curve, it can be

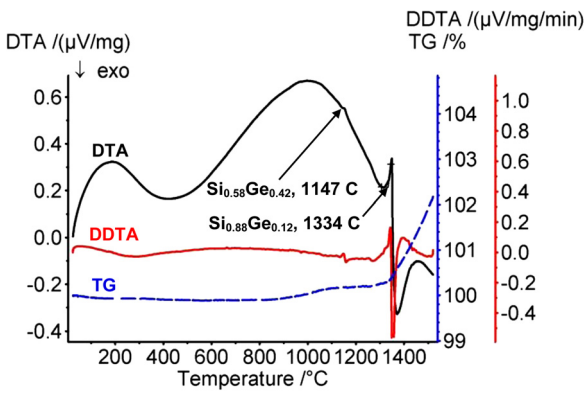

FIG. 2. DTA, DDTA, and TG data of the sample.

inferred that $Si_{0.88}Ge_{0.12}$ and $Si_{0.58}Ge_{0.42}$ alloys have been formed instead of the expected $Si_{0.8}Ge_{0.2}$ alloy.

It was hypothesized that the alloying to the nominal composition had not been completed after the last ball milling step. That is, the microstructure included a wide range of chemical compositions consisting of silicon and germanium. As a result of annealing at 1100 °C, liquation of Ge-rich alloy regions having solidus temperatures lower than 1100 °C produces a Ge-rich liquid and micro-segregated Si-rich solid regions. Since the initial powder mixture composition was Si-rich ($Si_{0.8}Ge_{0.2}$), the amount of Ge-rich regions is not considerable and no typical evidence of liquation like powder spoiling was observed. According to the phase diagram, all materials formed within the composition range of $Si_{0.17}Ge_{0.83}$ to $Si_{0.5}Ge_{0.5}$ provide a solid co-existing with liquid of $Si_{0.17}Ge_{0.83}$ composition at 1100 °C. This solid-liquid mixture and the liquids formed due to liquation of alloys with the Si contents less than 17 at. % form a single-phase liquid with a content less than 17 at. % at 1100 °C. Clearly, solidification of the formed liquid leads to regions with a high Ge concentration with severe micro-segregation and inhomogeneity, due to the low solidus temperatures compared with the annealing temperature at 1100 °C. The Ge content of these Ge rich regions is expected to reduce toward the equilibrium ratio of $Si_{0.8}Ge_{0.2}$ by subsequent milling. However, even after a long milling, there may still remain phases deviated from the equilibrium value. During sintering at 1200 °C, similar liquation of Ge-rich alloy regions having solidus temperatures lower than 1200 °C again may occur, forming another phase separation including a Ge-rich liquid and a Si-rich solid region. Finally, a typical dual-phase structure of $Si_{0.88}Ge_{0.12}$ and $Si_{0.58}Ge_{0.42}$ composition is developed. Such a heterogeneous phase was observed in the DTA data of many of our other hot pressed $Si_{0.8}Ge_{0.2}$ samples.

Although the TG graph of polycrystalline sample does not show any significant changes in mass in the whole temperature range, there is a small increase of mass after reaching the melting point. The mass increases approximately 2%–3% in temperatures higher than the melting point which may be associated to the oxidation of the sample. Due to the enhanced surface area in nanostructured sample, large amount of oxygen can be absorbed and react with the material increasing the mass at high temperatures.

It is difficult to detect the existence of the two phases of $Si_{0.88}Ge_{0.12}$ and $Si_{0.58}Ge_{0.42}$ from the XRD data as the diffraction peaks of these phases are close to those of $Si_{0.8}Ge_{0.2}$. The 2θ values for the diffraction lines of $Si_{0.88}Ge_{0.12}$ are 0.04°–0.08° more than those of $Si_{0.8}Ge_{0.2}$, and the 2θ values for $Si_{0.58}Ge_{0.42}$ are 0.13°–0.24° smaller. Therefore, their existence results in broadening of the $Si_{0.8}Ge_{0.2}$ lines, which makes it difficult to be distinguished from other sources of broadening such as residual stress, grain size, and the instrument. In addition, the phase heterogeneity of the alloy cannot be detected by Rietveld refinement either as Si and Ge can form a continuous solid solution; hence, many various phases can be formed that are unknown for this analysis. However, the data from the DTA would reveal the existing phases that can be input to the Rietveld refinement for further analysis.

The SEM micrograph of the nanostructured sample is shown in Figure 3. The image indicates that the grain sizes in nanostructured sample have different sizes mostly in the range of 10–100 nm. The grain size plays an important role in charge transport properties affecting the thermal properties of the sample. The charge carrier mean free paths (MFP) in $Si_{1-x}Ge_x$ is in the range of 1–5 nm while the phonon MFP is mostly in the range of 1–100 nm.[3,11] It means that the grains in the nanostructured sample are larger than the charge MFPs and smaller than the phonon MFP. Therefore, the grain boundaries (GBs) scatter phonons in a significantly higher rate than electrons. This effect reduces the thermal conductivity more than the electrical conductivity.

Figure 4 shows the thermoelectric properties versus temperature for nanostructured sample. The thermoelectric properties of single crystalline $Si_{0.8}Ge_{0.2}$ (Ref. 24) previously used in RTGs is also plotted for comparison. The room temperature electrical conductivity of the nanostructured sample is 560 S/cm which is significantly lower than that of RTG sample. This can be associated with both lower carrier concentration and lower charge carrier mobility. However, this difference reduces at high temperatures due to the dominancy of the acoustic phonon scattering mechanism compared with the GB scattering.[6] Comparison of the Seebeck coefficient of the nanostructured sample with that of the RTG sample confirms that the nanostructured sample has lower carrier concentration.

Although nanostructuring process can reduce the thermal conductivity via the increase of the interfaces, it can also reduce the concentration of the active dopants and increase the thermal instability of the structure. It has been shown that nanostructuring leads to the precipitation of boron at the grain boundaries, which reduces the carrier concentration and consequently the electrical conductivity.[6,25]

The increase of the thermal conductivity at high temperature is due to the ambipolar effect. It is seen that this effect is weaker in the nanostructured sample compared with that of the RTG sample. This can be associated with the effect of the existence of two different phases of $Si_{1-x}Ge_x$ in this sample. The dominant phase of $Si_{0.88}Ge_{0.12}$ has a larger band gap than $Si_{0.8}Ge_{0.2}$, which results in smaller ambipolar thermal diffusion.

Temperature dependence figure-of-merits of both samples are shown in Figure 5. The maximum figure-of-merit is 0.7 at 950 °C for the nanostructured sample. The benefit of

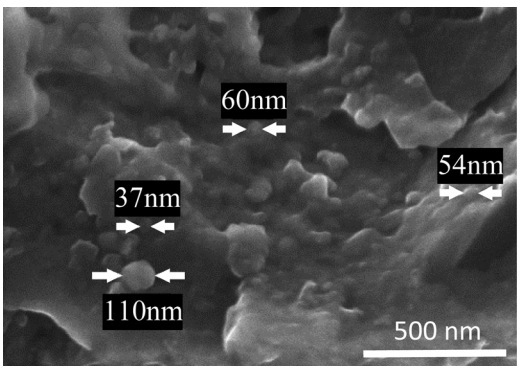

FIG. 3. SEM micrograph of the nanostructured silicon germanium.

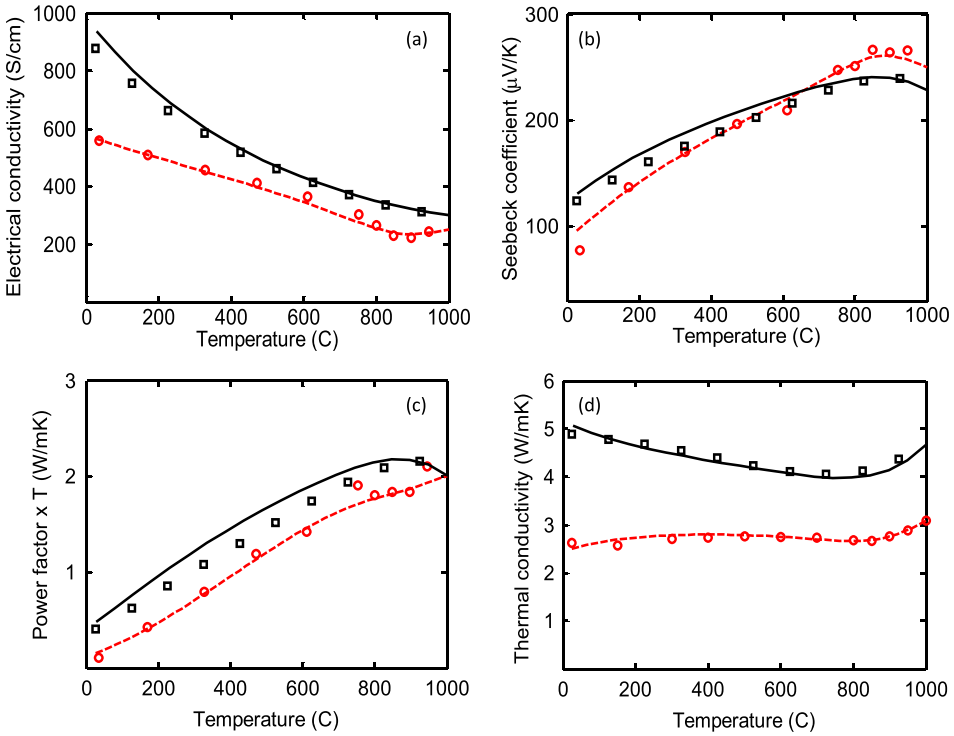

FIG. 4. (a) Electrical conductivity, (b) Seebeck coefficient, (c) power factor times temperature, and (d) thermal conductivity versus temperature for nanostructured silicon germanium (circles) compared with single crystalline silicon germanium used in RTG's.[24] Symbols are experimental data and solid lines are the theoretical modeling.

nanostructuring is obviously seen especially at high temperature ZT values, which is the operating temperature for this material system.

Theoretical modeling of the thermoelectric properties for both the nanostructured and crystalline samples is shown in Figures 4 and 5 along with the experimental data. The modeling process is described in previous works.[3,6,25] Here, the same procedure with similar material parameters was followed to calculate the thermoelectric properties. As it is shown, there is a good agreement between the theoretical and experimental data. The fitting process of the Seebeck coefficient, electrical, and thermal conductivities leads to crystallite size and interface potential parameters. The experimental results were explained with the theory assuming the average grain size of 27 nm and grain boundary potential of 170 meV. It is noted that the fitting to the experimental data was possible when the combination of the two different phases of $Si_{0.88}Ge_{0.12}$ and $Si_{0.58}Ge_{0.42}$ was considered in the calculations. For this purpose, the thermoelectric properties of the mixed phase system were calculated from those of the individual phases using the following equations: $\sigma = x\sigma_1 + (1-x)\sigma_2$, $\kappa = x\kappa_1 + (1-x)\kappa_2$, $S = x\sigma_1/\ \sigma S_1 + x\sigma_2/\sigma S_2$, in which σ_i, κ_i, and S_i are the electrical conductivity, thermal conductivity, and Seebeck coefficient of the different phases ($i = 1, 2$), respectively, and x is the volume fraction of $Si_{0.88}Ge_{0.12}$. $x = 0.73$, which was calculated knowing that the starting materials were weighted according to $Si_{0.8}Ge_{0.2}$, i.e., $0.866x + 0.55(1-x) = 0.779$. 0.866, 0.55, and 0.779 are the Si volume fractions in $Si_{0.88}Ge_{0.12}$, $Si_{0.58}Ge_{0.42}$, and $Si_{0.8}Ge_{0.2}$, respectively. Combining the values of the Seebeck coefficient, electrical and thermal conductivity of $Si_{0.88}Ge_{0.12}$ and $Si_{0.58}Ge_{0.42}$ phases according to these equations could fit the experimental data of the nanostructured sample.

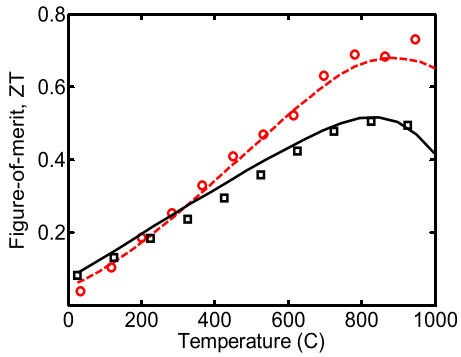

FIG. 5. Figure-of-merit as a function of temperature measured for nanostructured silicon germanium (circles) compared with the single crystalline $Si_{0.8}Ge_{0.2}$ used in RTG's. Solid lines show numerical modeling data.

The thermal conductivity components for the nanostructured and RTG samples are shown in Figure 6. As it is shown in Figure 6(a), the lattice part of the thermal conductivity is larger in $Si_{0.88}Ge_{0.12}$. The effect of alloy scattering reduces the thermal conduction; hence, with more Ge content, the lattice thermal conductivity decreases. The bipolar part of thermal conductivity of $Si_{0.58}Ge_{0.42}$ is higher than that of $Si_{0.88}Ge_{0.12}$ indicated by the higher slope of the thermal conductivity increase at high temperatures in this phase. Overall, it can be concluded that the presence of the dominant phase of $Si_{0.88}Ge_{0.12}$ alloy reduces the bipolar thermal conductivity, which is also observed in the thermal conductivity comparison of Figure 4(d).

Figure 7 shows the comparison of the figure-of-merit, ZT, of the three different phases of $Si_{0.58}Ge_{0.42}$, $Si_{0.88}Ge_{0.12}$, and the $Si_{1-x}Ge_x$ composed of $Si_{0.88}Ge_{0.12}$ (73 vol. %) and $Si_{0.58}Ge_{0.42}$ (27 vol. %). The three compositions have approximately similar ZT at low temperatures ($T < 700\,^{\circ}C$). At higher temperature, the ZT variation is strongly affected by the bipolar thermal conductivity and the bipolar effect on Seebeck coefficient. The $Si_{0.88}Ge_{0.12}$ phase has larger ZT, which is mainly due to smaller bipolar effect resulted from

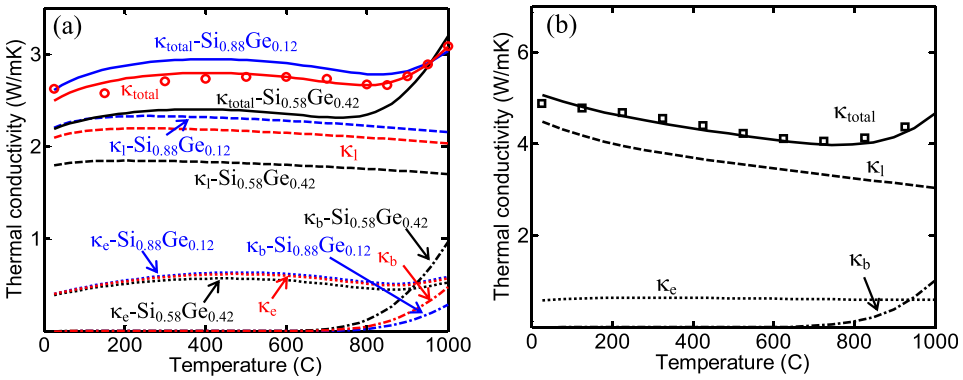

FIG. 6. Thermal conductivity components for (a) nanostructured and (b) crystalline silicon germanium.

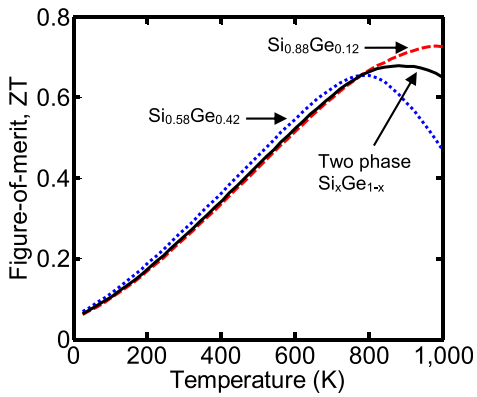

FIG. 7. Thermoelectric figure-of-merit versus temperature for three compositions of $Si_{0.58}Ge_{0.42}$ (dotted), $Si_{0.88}Ge_{0.12}$ (dashed), and $Si_{1-x}Ge_x$ (solid) composed of $Si_{0.88}Ge_{0.12}$ (73 vol. %) and $Si_{0.58}Ge_{0.42}$ (27 vol. %).

its larger bandgap. The ZT of the composite phase is between the ZT of the two constituent phases. This is in agreement with the previous theoretical predictions of the composite materials that the highest ZT of a composite material cannot reach to higher than the maximum ZT of the constituent components.[26] It should be noted that this prediction is based on classical theory and neglects the nanoscale effects in deriving this conclusion.

CONCLUSION

Nanostructured thermoelectric $Si_{0.8}Ge_{0.2}$ alloys were synthesized via high energy ball milling and hot-press sintering. The thermal and transport properties of the prepared sample were studied and compared with the conventional $Si_{0.8}Ge_{0.2}$ alloy used in RTGs. The theoretical modeling based on Boltzmann transport equations in relaxation time approximation framework was fitted to the experimental data. It was found that the Ge content has an essential role in thermoelectric properties of $Si_{1-x}Ge_x$ especially at high temperatures. In order to evaluate the actual phases developed in the $Si_{0.8}Ge_{0.2}$ structure, differential thermal analysis and thermogravimetery data of the synthesized sample were investigated in detail and compared with the X-ray diffraction data. We found that although x-ray diffraction results did not evidently show the presence of the different phases in the nanostructured sample, the DTA data taken over the temperature range of room temperature to 1500 °C indicated the presence of two different phases, none of which being the anticipated $Si_{0.8}Ge_{0.2}$ phase. Even though the amount of Ge was 20 at. % in the starting material, the dominant phase was $Si_{0.88}Ge_{0.12}$ along with a small amount of $Si_{0.58}Ge_{0.42}$. The effect of the smaller Ge content in the former phase appeared in reducing the Seebeck coefficient and the thermal conductivity at high temperatures.

The DTA results were further studied by theoretical modeling. In order to fit the experimental data, a two component $Si_{1-x}Ge_x$ structure with $x = 0.12$ and $x = 0.42$ was assumed in the theoretical modeling. The agreement between the theory and experiment confirmed the presence of the two phases and signified the effect of the variation in Ge content. In $Si_{0.8}Ge_{0.2}$ alloy, at high temperature, the bipolar effect in the thermal conductivity and the Seebeck coefficient is significant. The bipolar effect decreases with the reduction of the Ge content due to its smaller band gap. However, the lattice thermal conductivity is also a function of the Ge content and is smaller for the phase with higher Ge content (up to approximately 50 at. % Ge (Ref. 15)). Nevertheless, the reduction of the bipolar effect at high temperature is significantly more than the increase of the lattice part of the thermal conductivity when x increases above 0.12. Also, since different phases of $Si_{1-x}Ge_x$ have a similar crystal lattice structure with small deviation of the lattice constant, it is possible to make multicomponent $Si_{1-x}Ge_x$ structures with coherent grain boundary interfaces[27] that can improve phonon scattering while having minimal effect on the charge transport. Therefore, a multicomponent phase of the $Si_{1-x}Ge_x$ may provide a route for further improving the thermoelectric properties of this material system, which can be a subject for the future studies.

ACKNOWLEDGMENTS

This report was partially based upon work supported by Air Force Office of Scientific Research (AFOSR) High Temperature Materials program under Grant No. FA9550-10-1-0010 and the National Science Foundation (NSF) under Grant No. 0933763.

[1]D. M. Rowe, *CRC Handbook of Thermoelectrics* (CRC Press, 1995).
[2]M. S. Dresselhaus, G. Chen, Z. F. Ren, J.-P. Fleurial, P. Gogna, M. Y. Tang, D. Vashaee, H. Lee, X. Wang, G. Joshi, G. Zhu, D. Wang, R. Blair, S. Bux, and R. Kaner, in *Proceedings of the MRS Fall Meeting, November 26–30, Boston, MA, 2007*, Paper No. U2.4 (invited paper presented by M. S. Dresselhaus).

[3]Z. Zamanipour, X. Shi, A. M. Dehkordi, J. S. Krasinski, and D. Vashaee, Phys. Status Solidi A **209**(10), 2049–2058 (2012).
[4]D. Vashaee and A. Shakouri, J. Appl. Phys. **101**, 053719 (2007).
[5]G. H. Zhu, H. Lee, Y. C. Lan, X. W. Wang, G. Joshi, D. Z. Wang, J. Yang, D. Vashaee, H. Guilbert, A. Pillitteri, M. S. Dresselhaus, G. Chen, and Z. F. Ren, Phys. Rev. Lett. **102**, 196803 (2009).
[6]Z. Zamanipour and D. Vashaee, J. Appl. Phys. **112**, 093714 (2012).
[7]A. Minnich, H. Lee, X. W. Wang, G. Joshi, M. S. Dresselhaus, Z. F. Ren, G. Chen, and D. Vashaee, Phys. Rev. B **80**, 155327 (2009).
[8]D. Vashaee, J. Christofferson, Y. Zhang, A. Shakouri, G. Zeng, C. LaBounty, and X. Fan, Microscale Thermophys. Eng. **9**(1), 99–118 (2005).
[9]X. Fan, G. Zeng, C. LaBounty, D. Vashaee, J. Christofferson, A. Shakouri, and J. E. Bowers, Proceedings of 20th International Conference on Thermoelectrics, pp. 405–408, 2001.
[10]M. Zebarjadi, G. Joshi, G. Zhu, B. Yu, A. Minnich, Y. Lan, X. Wang, M. Dresselhaus, Z. Ren, and G. Chen, Nano Lett. **11**(6), 2225–2230 (2011).
[11]N. Satyala and D. Vashaee, Appl. Phys. Lett. **100**, 073107 (2012).
[12]N. Satyala and D. Vashaee, J. Appl. Phys. **112**, 093716 (2012).
[13]P.-E. Hellberg, S.-L. Zhang, F. M. d'Heurle, and C. S. Petersson, J. Appl. Phys. **82**, 5773 (1997).
[14]S. J. Kilpatrick, R. J. Jaccodine, and P. E. Thompson, J. Appl. Phys. **81**, 8018 (1997).
[15]J. Garg, N. Bonini, B. Kozinsky, and N. Marzari, Phys. Rev. Lett. **106**, 045901 (2011).
[16]M. N. Tripathi and C. M. Bhandari, J. Phys.: Condens. Matter **15**, 5359–5370 (2003).
[17]B. Abeles, Phys. Rev. **131**, 1906 (1963).
[18]C. Bera, M. Soulier, C. Navone, G. Roux, J. Simon, S. Volz, and N. Mingo, J. Appl. Phys. **108**, 124306 (2010).
[19]H. Stöhr and Z. W. Klemm, Z. Anorg. Allg. Chem. **241**, 305–323 (1954).
[20]R. Ferro and A. Saccone, Thermochim. Acta **418**, 23–32 (2004).
[21]P. J. Haines, *Thermal Methods of Analysis, Principles, Applications and Problems*, 1st ed. (Springer, 1995), pp. 63–122.
[22]P. Scherrer, "Bestimmung der größe und der inneren struktur von kolloidteilchen mittels röntgenstrahlen," Göttinger Nachrichten Math. Phys. **2**, 98–100 (1918).
[23]R. W. Olesinski and G. J. Abbaschian, in *Binary Alloy Phase Diagrams*, 2nd ed., edited by T. B. Massalski (Materials Information Soc., Materials Park, Ohio, 1990), Vol. 2.
[24]G. Joshi, H. Lee, Y. Lan, X. Wang, G. Zhu, D. Wang, R. W. Gould, D. C. Cuff, M. Y. Tang, M. S. Dresselhaus, G. Chen, and Z. Ren, Nano Lett. **8**(12), 4670–4674 (2008).
[25]Z. Zamanipour, J. S. Krasinski, and D. Vashaee, J. Appl. Phys. **113**, 143715 (2013).
[26]D. J. Bergman and O. Levy, J. Appl. Phys. **70**, 6821 (1991).
[27]H. Liu, Z. Zheng, D. Yang, X. Ke, E. Jaatinen, J. C. Zhao, and H. Y. Zhu, ACS Nano **4**(10), 6219–6227 (2010).